REVIEW

doi:10.1038/nature10381

Synthesis, assembly and applications of semiconductor nanomembranes

J. A. Rogers[1], M. G. Lagally[2] & R. G. Nuzzo[3]

Research in electronic nanomaterials, historically dominated by studies of nanocrystals/fullerenes and nanowires/nanotubes, now incorporates a growing focus on sheets with nanoscale thicknesses, referred to as nanomembranes. Such materials have practical appeal because their two-dimensional geometries facilitate integration into devices, with realistic pathways to manufacturing. Recent advances in synthesis provide access to nanomembranes with extraordinary properties in a variety of configurations, some of which exploit quantum and other size-dependent effects. This progress, together with emerging methods for deterministic assembly, leads to compelling opportunities for research, from basic studies of two-dimensional physics to the development of applications of heterogeneous electronics.

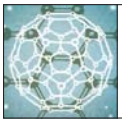

Semiconductor nanomembranes (NMs) are monocrystalline structures with thicknesses of less than a few hundred nanometres and with minimum lateral dimensions at least two orders of magnitude larger than the thickness. They differ from thin films in that they exist as free-standing, isolated forms at some critical stage in their growth or processing, or in their final, device-integrated forms. Because NMs offer many features that cannot be reproduced in other material formats, they are of central importance to a rapidly expanding frontier in nanoscience and technology. The origins of work on NMs can be traced back nearly thirty years to exploratory research on cadmium-based nanocrystals[1] and spherical fullerenes[2]. Studies of these and other 'zero-dimensional' materials evolved to include nanowires and carbon nanotubes[3], partly because it is comparatively easy (although still difficult) to form electrical contacts to such 'one-dimensional' structures. Although diverse types of semiconductor device are possible with individual wires/tubes, their practical application in high-yield, scalable systems faces formidable engineering challenges in assembly and other aspects of manufacturing. Materials in NM formats avoid these limitations, because their two-dimensional (2D) geometries are directly compatible with established device designs and processing approaches from the semiconductor industry, building naturally on decades of research in thin-film growth, patterning and processing. NMs also have finite-size and quantum characteristics in their electronic, phononic and optical properties, and have unique mechanical features, with effects related to shape distortions and folding of sheets, not found in zero- and one-dimensional materials. NMs can be made uniformly and repeatably (in size, shape, surface orientation, thickness and surface roughness) by 'top-down" methods used in semiconductor device manufacture.

Many advanced materials have begun to be studied in this format. These include a wide variety of inorganic materials, from those as common as silicon to esoteric layered compounds[4–6], as well as a rapidly growing range of forms of conjugated carbon[7–9], not limited to graphene. Sophisticated methods are becoming available for manipulating NMs with thicknesses of as little as a fraction of a nanometre and with lateral dimensions of up to many square centimetres, at high throughputs and yields[10–12]. NMs can be distributed over large areas, folded into various shapes[13–16] and wrapped onto curvilinear surfaces[17]. Advanced electronic and optoelectronic devices have been reported, each with a unique combination of operating speed[18], heterogeneous layout[19], flexible design[20,21], three-dimensional (3D) form[17,19] and other features that would be difficult or impossible to achieve with existing bulk materials technologies or with zero- or one-dimensional nanomaterials. These advances motivate the present Review of approaches to synthesis, assembly, and device integration for inorganic and organic NMs, excluding graphene, with an emphasis on challenges and future opportunities.

Inorganic nanomembranes

Single-crystalline inorganic semiconductor NMs with thicknesses that match length scales of important physical processes (a few hundred nanometres or less) offer opportunities in basic and applied research, as well as in technology, as suggested by recent demonstrations of practical devices that offer operational features unavailable with bulk materials. Figure 1 illustrates representative examples of NM properties in mechanics, electronics, thermoelectrics and photonics. In the first instance (Fig. 1a), the extremely small thicknesses of NMs (down to ~2 nm for silicon) lead to flexural rigidities that can be more than fifteen orders of magnitude smaller than those of bulk wafers (~200 μm) of the same materials[22]. The resulting values are so small, in fact, that they qualitatively change the nature of the material to allow otherwise impossible, non-planar geometries and multilayer integration options. The latter capabilities arise from the combined effects of low rigidities and energy release rates for thermally driven delamination that decrease linearly with thickness[23]. As a consequence, NMs conform and bond robustly to nearly any surface, thereby enabling them to be stacked onto one another or onto foreign hosts to yield unusual, heterogeneous systems that cannot be achieved with wafer-bonding technologies or epitaxy. Such stacking can lead to unusual electronic, electromechanical, thermoelectric, optoelectronic, optomechanical and photonic behaviour.

Sufficient thinness yields the 2D physics of quantum confinement, even in simple, single-layer NMs, with important implications for electronic transport. Figure 1b shows, as an example, the splitting of the conduction-band-minimum valley of silicon into subbands as a function of the thickness of the NM, for two orientations[24]. The right-hand plot shows how NM roughness affects the 2D density of states for these quantum-confined NMs[24]. A related phenomenon is the extremely high sensitivity

[1]Department of Materials Science and Engineering, University of Illinois, Urbana, Illinois 61801, USA. [2]University of Wisconsin-Madison, Madison, Wisconsin 53706, USA. [3]Department of Chemistry, University of Illinois, Urbana, Illinois 61801, USA.

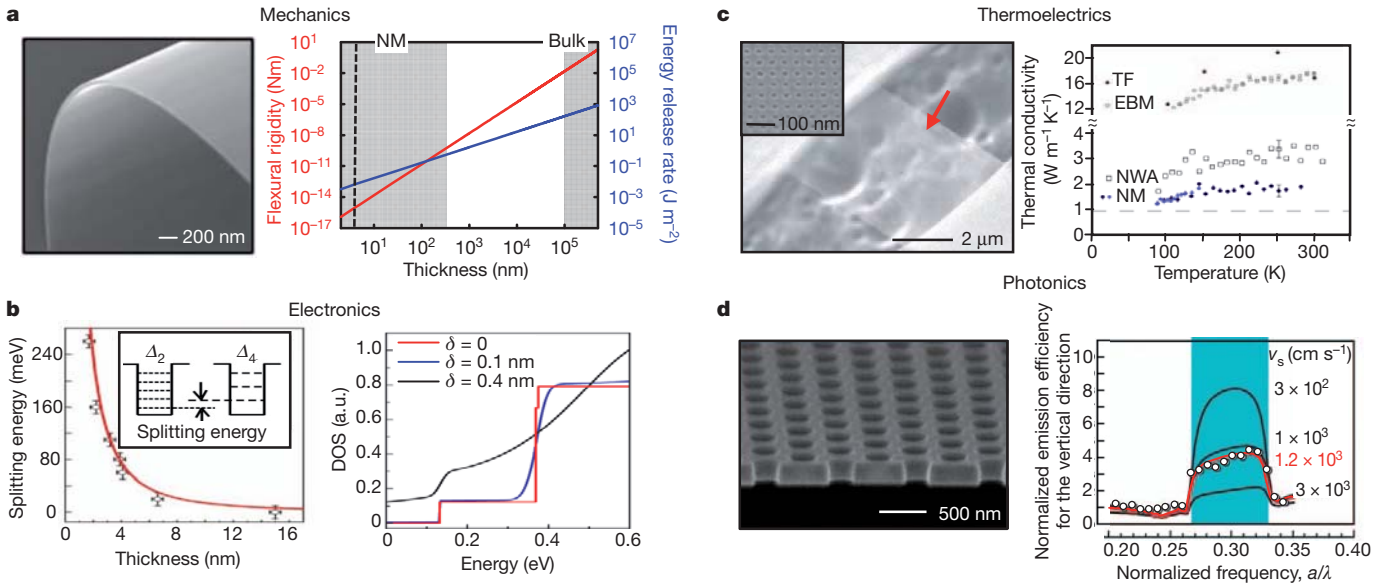

Figure 1 | Unique physical properties in NMs. **a**, NMs have exceptionally high degrees of bendability, as illustrated in the scanning electron microscope (SEM) image. The flexural rigidity of a 2-nm-thick, silicon NM is ~10^{15} times smaller than that of its bulk wafer counterpart (200 μm thick), as illustrated in the red curve of the graph (dashed line at 2 nm). Related mechanics allows bonding of NMs to nearly any surface. Here energy release rates associated with opening of interfaces between NMs and supporting substrates decrease linearly with thickness. The blue line represents calculations for silicon NMs bonded to sheets of polyimide at room temperature, and then heated to 300 °C. **b**, Electronic confinement effects in silicon NMs lead to splitting of the conduction band valleys (Δ) for the (001) orientation (left) with representative 1-s.d. error bars. Here the surface roughness (δ) strongly affects the 2D density of states[24] (DOS; right). a.u., arbitrary units. **c**, Phonon confinement in NMs offers opportunities for manipulating heat flow, to optimize figures of merit in thermoelectrics. The image shows a suspended silicon NM (22 nm thick; red arrow) perforated with arrays of nanoholes (diameter, ~10–15 nm; period, ~35 nm) that scatter phonons, thereby frustrating thermal transport[26]. The data compare such structures (NM) with arrays of nanowires (NWA; 28 nm wide, 20 nm thick), coarsely patterned NMs (EBM; square mesh with period of 385 nm, 22 nm thick) and uniform NMs (TF; 25 nm thick), with representative 1-s.d. error bars[26]. **d**, Photon confinement in NMs allows for low-threshold lasers. The SEM image shows a photonic crystal that consists of an array of nanoholes (period, ~500 nm) in a GaInAsP NM (245 nm thick), which is designed to suppress rates of spontaneous emission and, simultaneously, to direct light into vertical modes[28]. The graph shows measurements[28] (symbols) of emission efficiency, normalized to the case without nanoholes, as a function of the ratio of the period of the array (a) to the emission wavelength (λ). The results indicate enhancements for a range of a/λ values. Calculations (solid lines) with various surface-recombination velocities (v_s) capture the trends[28]. The blue region corresponds to the location of the photonic bandgap.

of charge transport to surface chemical condition, which also modifies the local band structure[25]. Other examples of dimensional effects in electronic properties are discussed below, in sections on synthesis and applications. The small thicknesses of NMs also strongly influence the behaviour of phonons and photons. Phonons can be used to increase key figures of merit (for example ZT) in thermoelectrics. NMs with arrays of nanoholes (Fig. 1c) that have lateral dimensions less than the mean free path of thermal phonons (~300 nm) and with thicknesses of about this value or less, produce strong backscattering effects that frustrate thermal transport, without reducing the electrical sheet resistance, owing to the comparatively shorter mean free paths of electrons and holes[26,27] (1–10 nm at high doping levels). Certain measurements of NMs with holes suggest thermal conductivities ~80 times smaller than values in bulk silicon, and enhancements in ZT of a factor of ~50 relative to NMs without holes[27]. Conceptually related effects of confinement can be used to advantage in optoelectronics. Some of the earliest examples involve lasers using NM-based photonic crystals that inhibit spontaneous emission by 94% and guide preferential emission into vertical modes, improving output efficiency by a factor of almost five[28,29] (Fig. 1d). The thicknesses of the NMs in such systems are typically a fraction of the emission wavelength to guarantee single-mode behaviour. Measurements and simulations shown in Fig. 1d capture these effects[28] and also underscore the critical role of surface recombination in NMs, as discussed below in the context of related applications.

Challenges common to all research efforts in NMs lie in the development of improved methods to synthesize NMs with precise dimensions and materials quality; to engineer structural features or distributions of strain in NMs to yield unusual charge, photon or phonon transport characteristics; to stack and bond NMs, with an emphasis on the control of surface/interfacial properties and on charge transport across bonded-NM interfaces; to deform NMs into unusual shapes for non-planar components, such as cylindrical microcavity lasers and stretchable, bio-integrated electronics; and to produce large numbers of NMs with precise geometries, efficiently and cost effectively, and assemble them in desired configurations at high throughputs. The following sections highlight exemplary recent advances and areas of future opportunity.

Synthesis

In a route similar to that used to create graphene from bulk pieces of graphite, inorganic NMs can be (and have been for many years) formed by chemical or mechanical exfoliation from solids that have naturally layered structures[4–6], such as the semiconductors MoS_2 (refs 4, 30, 31), $Sr_2Nb_3O_{10}$ (ref. 5), GeS (ref. 32) and GeSe (ref. 32). Recent work indicates that confinement effects in single-layer NMs of MoS_2 (Fig. 2a) lead to direct bandgaps, unlike the indirect gaps of bulk samples[31]. Transistors that incorporate these NMs show field-effect mobilities greater than those that use graphene structured in nanoribbon geometries required to create a bandgap for efficient switching behaviour[31]. As a result, exfoliated NMs are of interest as ultrathin alternatives to graphene for active materials in next-generation electronics, where interband tunnelling might be used to improve performance in low-power devices further.

Although exfoliation yields large numbers of NMs from certain classes of semiconductors such as MoS_2, additional methods are needed to control their dimensions and shapes, and to manipulate them for integration into systems. A synthetic strategy that addresses these requirements and expands the materials options involves the release of NMs from bulk semiconductors that are not naturally layered, by use of specialized anisotropic etching procedures. For example, defining trenches on the surfaces of silicon wafers with {111} orientations, and

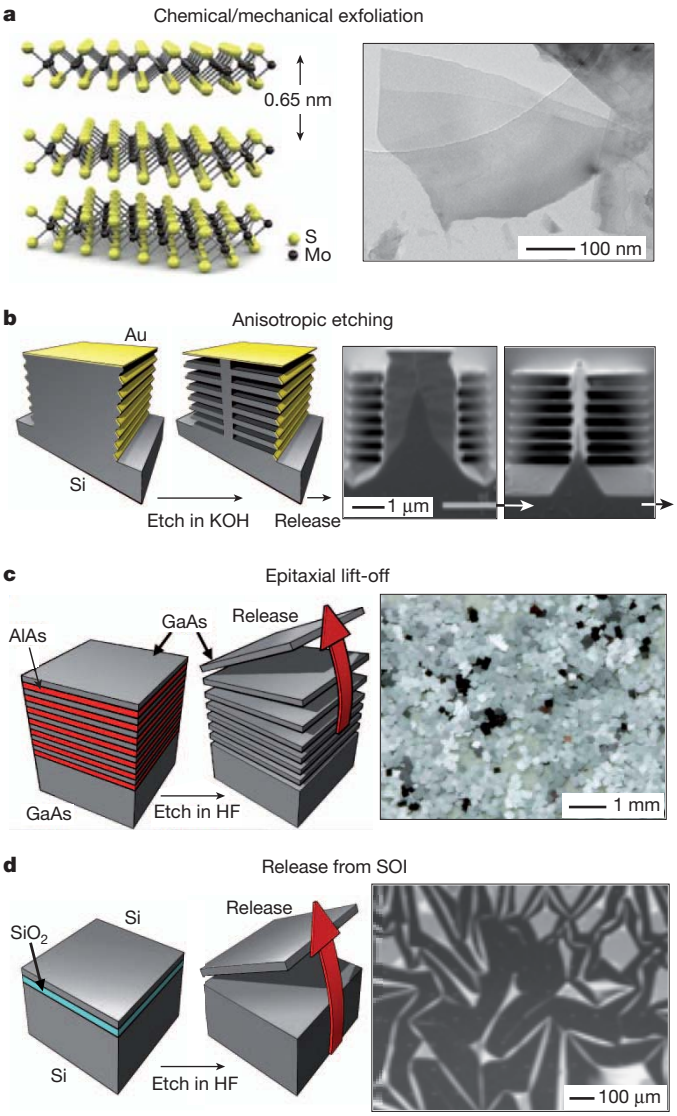

Figure 2 | Representative routes for synthesizing inorganic monocrystalline semiconductor NMs. **a**, Atomic structure of MoS_2, showing its layered configuration[31]. Chemical or mechanical exfoliation of this material yields single-layer NMs (0.65 nm thick), as shown in the transmission electron microscope image on the right[30]. **b**, Process for generating multilayer stacks of silicon NMs from a bulk wafer by anisotropic etching. Patterned features of etch resist (gold) on the structured sidewalls of vertically etched trenches allow access of an anisotropic wet chemical etchant only to certain regions of the silicon. Etching releases silicon NMs (~100 nm thick), as shown at two intermediate times in the cross-sectional SEM images on the right[35]. **c**, Epitaxial multilayer assembly of GaAs and aluminium arsenide (AlAs) grown on a GaAs wafer[36]. Etching vertically through the thickness of the stack and then immersing the structure in hydrofluoric acid leads to the selective removal of the AlAs layers. Complete undercut etching releases large numbers of GaAs NMs. The SEM image shows a collection of GaAs membranes formed using this process[36]. **d**, Release of a silicon NM from a SOI wafer. Etching vertically through the top silicon layer exposes the underlying SiO_2 layer, allowing its removal by etching in hydrofluoric acid. The optical image on the right shows a wrinkled, but completely single-crystal, silicon NM (~50 nm thick) formed in this manner that can then be transferred to a new host, where it will flatten and bond[10].

then patterning their side walls with etch resists provides a starting point for the anisotropic removal of material along the ⟨110⟩ directions using solutions of potassium hydroxide[33,34]. The process (Fig. 2b) releases stacks, and, with minor modifications, essentially bulk-like numbers of NMs[35]. An appealing aspect of this synthesis is that lithography defines the lateral dimensions of the NMs and their spatial positions across the wafer, thereby rendering them compatible with methods for integration described below. Cycles of thermal oxidation and etching can reduce the thicknesses and passivate the interfaces.

Methods that offer atomically smooth surfaces and enhanced dimensional control over large areas begin with epitaxial growth to form releasable multilayer assemblies. For example, stacks of gallium arsenide (GaAs) films separated by aluminium gallium arsenide (AlGaAs) yield large numbers of GaAs NMs on selective removal of the AlGaAs with hydrofluoric acid[36]. This process provides significant cost and throughput advantages over related approaches that release only single layers[37–39], owing to more efficient use of the systems for epitaxial growth and the supporting substrates[36]. Fig. 2c shows an illustration of the process and an image of a deposit of released GaAs NMs formed by casting from a solution suspension[36]. Similar multilayers can yield, from a single stack, NMs for multifunctional integrated systems of radio-frequency electronics, photodetectors, light emitters and solar cells[36,40]. Epitaxial layers for passivation can be grown directly, to form an integral part of the NM. Multimaterial structures, such as those of GaAs with self-assembled quantum dots of indium arsenide (InAs) as embedded light emitters, are also possible, for applications in optoelectronics[41]. The thin geometries of NMs can be important in these types of epitaxial synthesis because they avoid the dislocations that occur in films thicker than the critical thickness for defect formation in strained layers[42]. Additionally, greater materials possibilities follow from the use of NMs as growth substrates, where modified lattice constants or strain symmetries, not achievable in bulk materials, can be exploited, as described below.

A complementary scheme that avoids the demands of epitaxy entirely uses layered materials formed by wafer bonding followed by polishing or controlled fracture. The most common example starts with a thin layer of silicon on silicon dioxide (SiO_2) supported by a silicon substrate, known as silicon on insulator[13,43–45] (SOI). Etching the buried oxide with hydrofluoric acid releases the top silicon layer as a NM (Fig. 2d). Commercially available SOI can be used to make silicon NMs with thicknesses down to 20 nm. Oxidation and etching can reduce the thickness to <2 nm, with uniformity greater than 0.3 nm (ref. 25). Other examples of SOI-like structures include group-IV analogues such as germanium on insulator, strained silicon on insulator and silicon–germanium (SiGe) on insulator, as well as III–V semiconductors and many other combinations[46–48].

Strain engineering and 3D nanoarchitectures

An intriguing aspect of the synthesis of NMs is the ability to modify structures by lithographic processing (Fig. 1c, d) or by introducing spatial distributions of strain. The latter offers great promise for the creation and investigation of new physical properties. The distinctive mechanical properties of NMs (see discussion above and Fig. 1a), allow this strain engineering. Strain changes the lattice constant, thereby creating new properties relative to the unstrained, but chemically identical, material. The ability to alter the strain, in magnitude, direction, spatial extent, periodicity, symmetry and/or nature, allows tuning of the intrinsic properties to such a degree that many are significantly modified, including band structure, charge carrier mobility, atomic transport, atomic defect structure, the self-assembly of quantum dots, piezoresistivity, and more complex phenomena such as electro-optical effects[49–51].

Lattice strain can be introduced by heteroepitaxial growth of materials with different lattice constants[13,44,52]. For example, in a trilayer of Si/SiGe/Si grown on SOI, the SiGe layer is compressively strained and the silicon layers are unstrained. When this trilayer is released, the SiGe layer shares its strain elastically with the silicon layers, with strain magnitudes of up to 1%. Strains in this range can cause significant changes in the band structure of silicon[50], such as to improve the performance of transistors on flexible polymers[53], and, if applied locally and periodically, to form strain-induced, single-element electronic heterojunction superlattices[49,54]. This elastic strain sharing, with appropriate processing, can be used to produce special defect-free semiconductors that cannot be realized in other ways[55], and, by taking advantage of differing crystal symmetries in the components of strained multilayer composites, to make entirely new

materials with crystal symmetries that do not exist in bulk form and cannot be created by heteroepitaxy alone[56].

Strain can also be introduced mechanically. Again, the distinctive mechanical properties of NMs are decisive in achieving novel properties. For example, it has recently become possible, because the conduction-band valleys shift by different amounts with strain, to stretch germanium NMs biaxially sufficiently to change germanium from an indirect-bandgap semiconductor to a direct-bandgap semiconductor[57]. This transformation allows use of germanium in light sources, thereby realizing the vision of group-IV-semiconductor integrated electronics and optics.

A related consequence of strain control is that the geometries of NMs can be engineered to yield 3D shapes, allowing device configurations and properties that would be impossible to achieve with bulk materials. Possibilities include tubes that can provide active growth platforms for cells[58], cylindrical microcavities that can serve as fluidic channels and optical sensors[59], and buckled structures that can respond elastically to large strains and can be used in stretchable electronics[45,60,61]. With appropriate engineering of strains in systems in which there is a strain gradient perpendicular to the layers, tubes, spirals, rings and other 3D nanoarchitectures can be achieved[13–16,44]. For isotropic elastic moduli, the bending, rolling or curling behaviour can be calculated using the classical Timoshenko formula[62]. In this case, a strained bilayer NM strip tends to roll (along its long direction) into a tube when the strip is wide or into a ring when the strip is narrow. A long narrow strip may, however, form a coil, owing to shear terms in the minimization of energy. Figure 3a illustrates the conditions. A tube will form if the width, W, of the strip is large relative to the radius of curvature determined by the bilayer strain, which is related to the circumference, L_0, of the tube. Beyond a critical angle, θ_c, determined by $W/L_0 = \sin(\theta_c)$, a long, strained NM strip will roll into a coil of radius R_0, which also is related to the radius of curvature determined by the bilayer strain. More varied shapes can form when the materials have elastically soft and hard directions. Figure 3b shows rolled-up tubes of GaAs NMs with embedded quantum wells, which have applications as an unusual type of optical resonator[63]. Fig. 3c shows spirals that form ribbon-shaped SiGe NMs[64]. The centre regions remain flat because they are attached to the underlying substrate. Lithographic patterning allows elaborate architectures that create many new design opportunities in semiconductor devices, as described in the section on applications below.

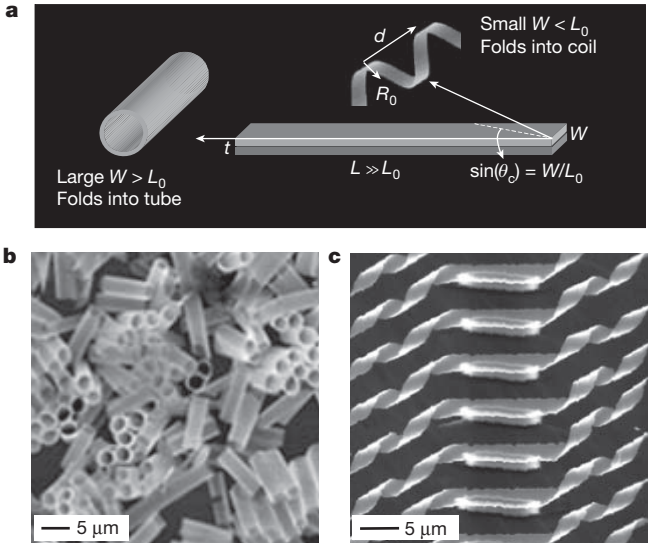

Figure 3 | Inorganic monocrystalline semiconductor NMs in non-planar configurations. a, Rolling and curling in a strained bilayer NM, illustrating the geometric parameters that determine the morphology: $L_0 = 2\pi R_0$ is the circumference of a tube that may form; L and W are the length and width of the strip, respectively; and t is its thickness. The critical angle for coil formation over tube formation is θ_c. The arrows indicate the folding direction[14]. **b**, SEM image of a collection of GaAs NMs with embedded quantum well structures. The tubular shapes form on release from the substrate, owing to strain in the epitaxial layers[63]. **c**, SEM image of an array of partly released spiral structures formed by SiGe (10 nm)/Si (7 nm)/Cr (20 nm) NMs attached at their centres to a silicon wafer[64].

Organic nanomembranes

The chemical diversity and unique properties of organic NMs make them an attractive complement to the inorganic materials described above. Graphene provides the most compelling existing example because of its superlative mechanical, thermal and charge transport properties, and the device opportunities, unavailable to bulk graphite[65], that it affords. These observations motivate work to explore other 2D carbon allotropes, such as those with *sp*- and sp^2-hybridized carbon (for example graphyne and graphdiyne) with similar, molecular-scale thicknesses[7–9,66,67]. These materials, as well as other more structurally and compositionally diverse organic NMs, are expected theoretically to offer bandgaps, mobilities and other electronic characteristics that are much different from those of graphene[7–9,66,67]. For example, calculations suggest that graphdiyne has a mobility as great as $\sim 10^5\ cm^2\ V^{-1}\ s^{-1}$ and a bandgap of ~0.5 eV (ref. 68), thereby making this type of NM attractive as a semiconductor for power-efficient, high-speed transistors, where unpatterned graphene NMs cannot be used because of their intrinsically semi-metallic nature.

The construction of 2D, ordered networks of carbon–carbon bonds in materials other than graphene remains a frontier challenge in chemistry[8,9]. Difficulties lie in the establishment of bonds with the necessary precision in high-molecular-mass systems that have the requisite solubility and avoid the propensity to aggregate[9,69]. As a result, present techniques of bulk, solution-phase synthetic chemistry typically limit the formation of organic NMs to lateral dimensions barely exceeding the molecular regime. An alternative scheme involves the assembly of molecular building blocks at interfaces, in the form of self-assembled monolayers (SAMs) or Langmuir–Blodgett films, to provide planar precursor films for NMs that form by reactions between the molecular constituents. Figure 4a illustrates the former process, and Fig. 4b shows an example of a 2,5-substituted dialkynylbenzene-bearing SAM on silica, catalytically crosslinked by alkyne metathesis to yield a highly conjugated carbon NM (a remarkably tough monolayer-thick sheet), capable of release and transfer to a silicon wafer for possible integration with established electronically active components[70]. Alternatively, crosslinking can be accomplished in related SAMs by low-energy electron bombardment[71]. For nitroaryl thiols on gold, this process forms a dense, crosslinked matrix in the aryl segments and elicits a reduction of the chain-end nitro substituents to amino groups. Detachment from the gold yields a NM that bears thiol groups on one face and amino groups on the other, with potential relevance for devices that demand different electronic interfaces on top and bottom. In Fig. 4c, the NM sits on a supporting grid; the colour arises from fluorescent labelling of the amino side. This synthesis also allows patterning by spatially modulating the electron dose, which has clear relevance for use in devices[72]. Pyrolysis yields metallic NMs that have conductivities similar to those found in graphitic forms of carbon[73], with immediate applications as conductive grids for transmission electron microscopy.

Although reported Langmuir–Blodgett and SAM techniques can yield macroscopic NMs in various forms, the absence of long-range coherence in the bonding configurations severely degrades charge transport characteristics. This challenge can be addressed with interfacial interactions templated by monocrystalline substrates. Recent work demonstrates the feasibility of this idea in the case of graphene-like NMs, in a manner that seems to be extendable to other organic NMs[74,75]. Figure 4d, e shows chevron-shaped graphene ribbons synthesized on a Au(111) crystal through the thermolytic condensation and cyclodehydrogenetic conversion of the molecular precursor 6,11-dibromo-1,2,3,4-tetraphenyltriphenylene[74]. These ribbons align and assemble along the direction of the corrugation of the herringbone reconstruction of the Au(111) substrate. Related approaches have yielded interesting classes of crystalline

monolayers from assemblies of molecules of 1,4-benzenediboronic acid, interlinked by the B–O–B bonds of the boroxine moiety[75]. Recent results suggest that other covalent organic frameworks can be synthesized using graphene as a templating substrate[76]. With additional work, these types of chemistry have great potential to yield the classes of monocrystalline organic NMs considered in this Review.

Single- and multilayer assembly

Systematic scientific studies benefit from, and engineering applications require, reliable techniques for integrating NMs into device or test structures. Materials created by bulk synthesis or by batch exfoliation from solids or surfaces can be assembled most readily through processes that start with suspensions of NMs in fluids[77–79], where adapted forms of ultracentrifugation, membrane filtration and chromatography offer means of separation, size selection and purification[80–82]. Langmuir–Blodgett techniques and controlled precipitation can yield thin-film-type assemblies, in single- or multilayer formats[77,80,81,83]. The resulting deposits can be transferred to substrates of interest for integration into devices as thin films. The levels of control in such solution-based processes can be enhanced through patterned surface functionalization, controlled fluid flows, capillarity or shape complementarity to guide the placement of individual NMs, using schemes originally developed for nanowires/nanotubes and for small-scale integrated circuits[84,85]. The intrinsically stochastic nature of these processes of guided self-assembly, however, imposes limits on the yields and the placement accuracy.

By contrast, NMs formed at interfaces that make controlled release possible can be manipulated using purely deterministic assembly techniques, with high yields and extreme accuracy in position, orientation and layout. Such capabilities are essential for all foreseeable applications in electronics, because of the requirement to integrate the NMs at specific locations in larger systems with submicrometre accuracy. The most well-developed approaches exploit forms of printing using soft, elastomeric stamps that allow manipulation of NMs without exceeding the critical strain levels for structural damage[10–12,36,43,86]. As an advanced example, Fig. 5a shows a structured stamp (blue) designed to allow pressure-modulated adhesion with two states, strong adhesion (ON) and weak adhesion (OFF), to facilitate retrieval and printing, respectively; here, the stamp is 'inked' with a thick platelet of silicon (green). (Temporary 'carrier' films of photoresist allow manipulation of NMs

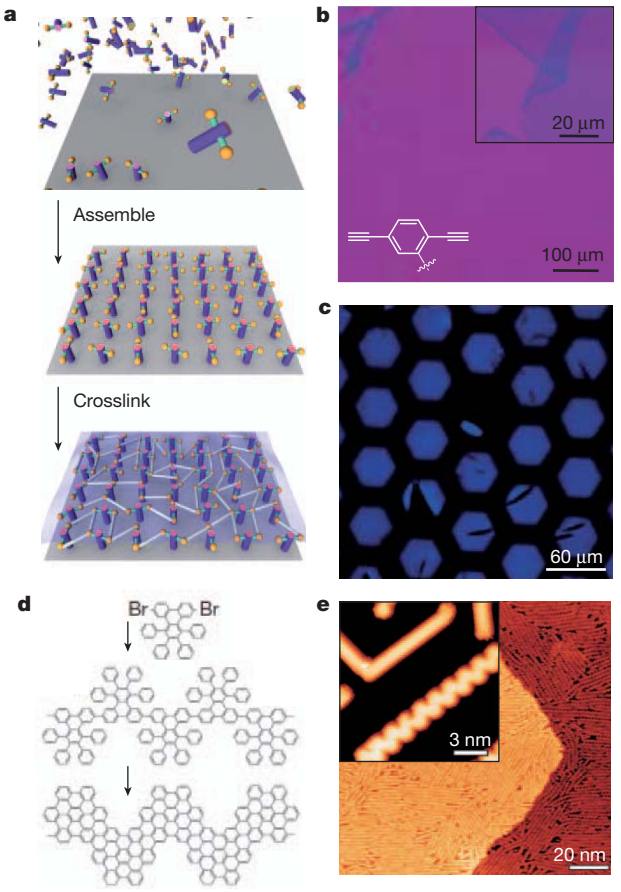

Figure 4 | NMs of conjugated carbon and their synthesis using interfacial methods. **a**, Approach to synthesis based on chemical crosslinking of a SAM[70]. **b**, Optical micrographs of a highly conjugated carbon NM synthesized by crosslinking a 2,5-substituted dialkynylbenzene SAM by alkyne metathesis, resting on a SiO_2/Si substrate[70]. A wrinkled region of the NM appears in magnified view on the top right. The chemical structure of the monomer appears on the bottom left. **c**, Fluorescence resonance energy transfer image of a ~1-nm-thick 'Janus' NM (blue) suspended over a supporting, hexagonal grid structure[71] (black). This NM, which has some tears and other defects, was formed by exposing a 4′-nitro-1,1′-biphenyl-4-thiol SAM to electrons at 100 eV and 50 mC cm^{-2}. **d**, Chemical synthesis of chevron-shaped graphene nanoribbon structures on Au(111), formed by thermolytic condensation and cyclodehydrogenetic conversion of the molecular precursor 6,11-dibromo-1,2,3,4-tetraphenyltriphenylene[74]. **e**, High-magnification (inset) and low-magnification (main image) scanning tunnelling microscope images of straight and chevron-shaped graphene nanoribbons on Au(111) synthesized in the manner illustrated in **d**[74].

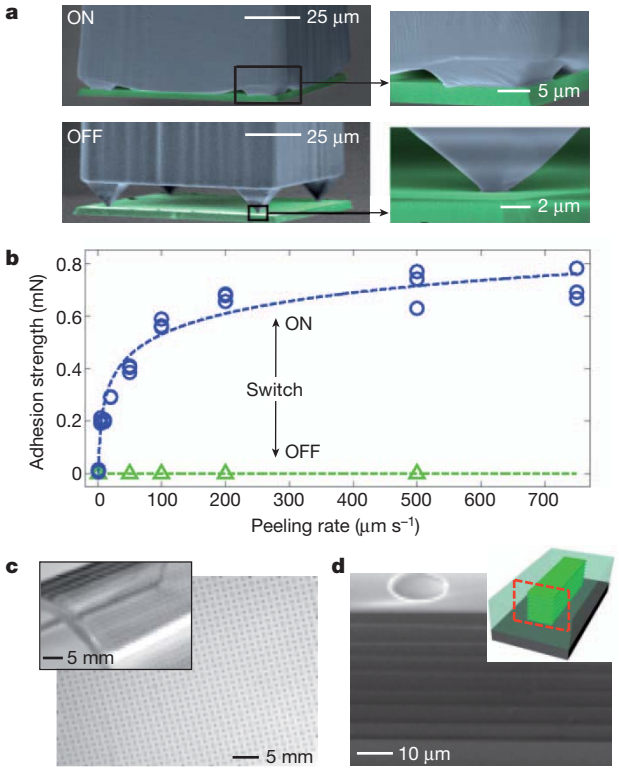

Figure 5 | Operation of elastomeric stamps for deterministic assembly of NMs, with examples of printed sparse arrays and multilayer assemblies. **a**, Colourized SEM images of a single post in an elastomeric stamp (blue) that uses soft, pyramidal relief features to provide strong adhesion in a collapsed state (ON) and weak adhesion in a retracted state[10] (OFF). Control of the applied pressure allows reversible switching between these two states. **b**, Measured adhesion strength in the ON and OFF states, as a function of peeling rate[10]. Viscoelastic effects in the elastomer lead to monotonic increases in adhesion with rate, with pronounced effects observable in the ON state. The dashed lines are guides for the eye. **c**, Sparse array of GaAs membranes (small black squares) assembled by printing onto a plate of glass (main image) and a bent sheet of plastic (inset)[40]. **d**, Cross-sectional SEM of an eight-layer stack of silicon NMs (each ~340 nm thick) separated by transparent layers of polymer. Inset, schematic; the red box outlines the cross-section shown in the main image.

with arbitrarily small thicknesses.) The data in Fig. 5b illustrate this switching capability, where both geometric[10] and viscoelastic[11] effects have important roles. Printing in single or multiple cycles can populate small or large areas of flat or curved substrates with NMs at any level of coverage, from full monolayers to sparse distributions in regular or irregular layouts. Figure 5c shows an organized collection of membranes of GaAs printed onto a flat plate of glass and a bent plastic substrate, starting from a dense array released from a GaAs wafer, using techniques similar to those of Fig. 2c[40]. Recent work indicates that it is even possible to print rolled-up NMs (Fig. 3b) using soft stamps[15].

These methods, and related ones that rely on hard stamps or releasable tapes, can be used with both inorganic and organic NMs to yield various configurations, including suspended 'bridge' and 'drumhead' geometries[10,70] for resonators in nanoelectromechanical systems, large-area, continuous sheets[87] for flat-panel displays, and unusual, hybrid-material constructs[88]. As an example of the last possibility, Fig. 5d shows a stack of eight silicon NMs, each separated by a transparent polymer film, for an application in multilayer optoelectronics where these layers support waveguide arrays for phase-controlled beam steering. Fully automated tools now exist for assembling these and related structures[36,40], with printing rates of up to millions of NMs per hour, or more, depending on the sizes and layouts. Yields of nearly 100% and placement accuracy better than 1 μm can be achieved with NMs having thicknesses in the near-atomic range, relevant for single-layer NMs[89,90], and areas of square centimetres or more.

Applications in electronics and optoelectronics

The synthesis and assembly techniques described above, coupled with the unique mechanics and confinement effects provided by NMs, provide diverse capabilities in electronics. The most intriguing areas of application are those that cannot be addressed with any other bulk, thin-film or nanomaterials technology. Advanced demonstration devices of this type have been reported, perhaps most significantly in the area of flexible and stretchable electronics. In these cases, NMs of silicon[18,21,53,60,91,92], GaAs (refs 36, 40, 93) or GaN (ref. 94) serve as active materials, mounted on plastic or rubber substrates and configured in mechanical layouts and 3D nanoarchitectures that allow bending, stretching, folding, twisting and other demanding modes of deformation without inducing damage or fatigue in the materials.

An emerging NM technology that exploits these features involves intimate coupling of electronics with biological tissues in ways that would otherwise be impossible[21,45,93]. Fig. 6a shows an example of this sort of bio-integrated device, in which a thin, flexible film supports an interconnected array of 288 actively multiplexed, amplified sensing electrodes[21]. The system includes more than 2,000 silicon NM transistors on a thin sheet of polyimide, in a waterproof format that non-invasively laminates onto the epicardial surface (porcine animal model shown here), like a piece of Saran wrap. The device performs temporal and spatial mapping of electrophysiology at unprecedented levels of speed and resolution, for diagnostic purposes in surgical procedures to treat arrhythmias and other forms of cardiac disease. The colour inset in Fig. 6a shows typical data. Related components can serve as advanced surgical tools or therapeutic devices, not only in cardiology but also in neurology and other areas.

Key performance attributes of the NM transistors in these systems are enhanced by layers of SiO_2 that passivate the surfaces of the silicon to facilitate charge transport. As a result, these circuits have performance comparable to analogous systems on SOI, with normalized current outputs[60] and switching speeds[92] that exceed those of systems based on organic semiconductors or films of quantum dots or nanowires. Such NMs can in fact provide a route to plastic radio-frequency electronics[95]. Fig. 6b shows gigahertz-frequency operation in silicon NM transistors on a sheet of polyethylene terephthalate[18]. This type of technology provides a radio-frequency electronics platform of interest not only for its unusual mechanics but also for its potential as a low-cost

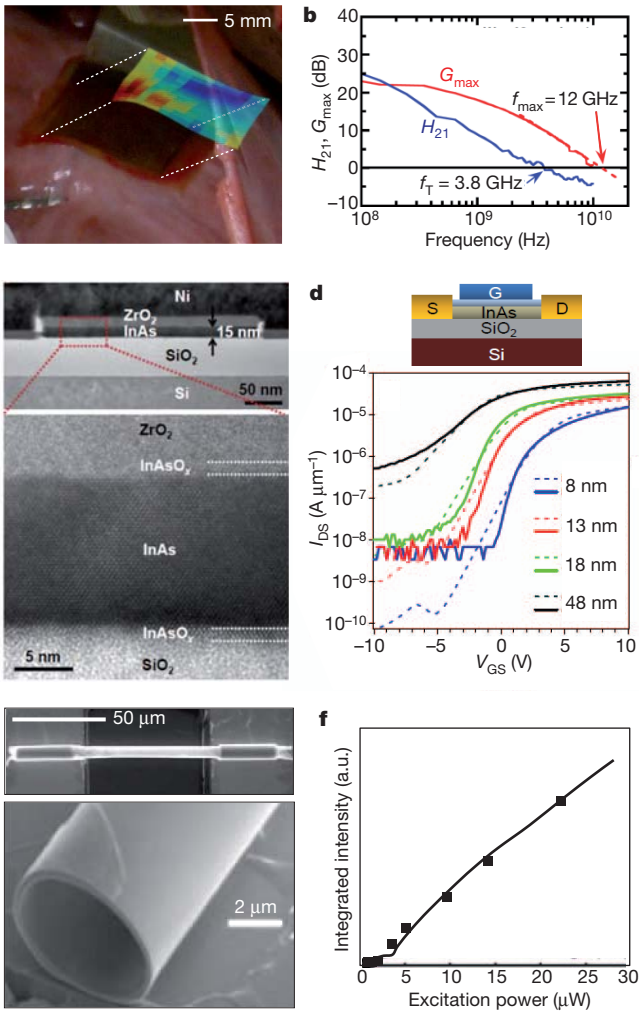

Figure 6 | NMs as active materials in unusual electronic and optoelectronic devices. **a**, Bio-integrated electronics for high-resolution mapping of cardiac electrophysiology in a porcine animal model, with applicability in humans[21]. The device consists of nearly three hundred independent measurement locations, with local amplifier circuits and multiplexers that collectively use more than 2,000 silicon NM transistors in a waterproof construction on a thin sheet of polyimide. The colour inset provides a representative map collected using this device. **b**, Small-signal current gain (H_{21}) and power gain (G_{max}) as functions of frequency for high-speed silicon NM transistors on a plastic substrate[18]. The results show limiting frequencies of 3.8 GHz for current gain (f_T) and 12 GHz for power gain (f_{max}). For power gain, the solid and dashed lines correspond to measurement and simulation, respectively. **c**, Cross-sectional transmission electron microscope images of a transistor that uses an InAs NM heterogeneously integrated on an oxidized silicon wafer, at moderate (top) and high (bottom) magnifications[96]. **d**, Measured (solid) and simulated (dashed) width-normalized drain–source currents (I_{DS}) as functions of gate–source voltage (V_{GS}) for transistors as in **c** with InAs NM thicknesses of 8, 13, 18 and 48 nm (ref. 96). A cross-sectional schematic of the transistor is shown at top. **e**, SEM images of a cylindrical microcavity laser formed with a NM (~50 nm thick, with two InGaAs/GaAs quantum dot layers and a pseudomorphic $In_{0.18}Ga_{0.82}As$ quantum well), at low (top) and high (bottom) magnifications[97]. **f**, Integrated output intensity as a function of excitation power (HeNe laser emission at 632.8 nm) for emission in an optically resonant mode with a wavelength of 1,240.7 nm (ref. 97).

alternative to conventional systems, which require semiconductor wafers as substrates.

In the devices of Fig. 6a, b, NMs overcome incompatibilities in processing and growth conditions between high-temperature active materials and low-temperature substrates, by exploiting the mechanics illustrated in Fig. 1a. A related advantage appears in the context of mainstream electronics in cases where integration by means of heteroepitaxial growth or wafer bonding is impossible because of mismatches in lattice constants

or coefficients of thermal expansion, respectively. For example, silicon NMs can be bonded directly to germanium substrates and vice versa, with narrow interfaces and high cross-interface electrical conductivity, which is challenging to achieve with bulk wafer-bonding techniques. Such unique capabilities make possible a range of group-IV optoelectronic and tunnelling devices in which charge transport across interfaces is essential[23].

Equally important in digital integrated circuits, but not typically requiring cross-interface transport, is joining compound-semiconductor NMs with silicon wafers, down to the level of individual devices. There the high mobilities and conductivities of InAs NMs, for instance, could help to overcome fundamental limitations on the speed and energy efficiency of silicon transistors. Figure 6c shows cross-sectional transmission electron micrographs of a transistor formed from an InAs NM printed onto a silicon wafer[96] using the techniques described in the previous section and the bonding mechanics illustrated in Fig. 1a. Figure 6d illustrates the transistor schematically and shows its current–voltage characteristics. Strong confinement effects allow orders-of-magnitude increases in switching ratios compared with bulk devices, mainly through improved electrostatic coupling to the gate, and reductions in the maximum currents due to a transition from 3D to 2D transport. Figure 6d shows trends as the thickness of the NM increases from 8 to 48 nm. Interfacial layers of $InAsO_x$, thermally grown onto the InAs NMs before device integration, are critically important in reducing the interfacial trap densities.

Passivated NMs can also be used to achieve radically different device geometries. As an example, Fig. 6e shows a cylindrical microcavity laser formed by stress-induced rolling of a GaAs/InGaAs NM with embedded, self-organized quantum dots as the gain medium[97]. As configured in a suspended state, the tube yields a cavity with excellent coupling of the maximum field intensity and the gain region. Minimal optical scattering and reduced non-radiative recombination at surface defects result from epitaxially smooth surfaces and effects of carrier confinement, respectively. The graph in Fig. 6f shows measured characteristics of the microcavity laser. Non-planar device designs represent an interesting alternative to the more widely explored microcavities based on photonic crystals, microdisks, micropillars and other geometries. These and other unique 3D nanoarchitectures allowed by NMs are also being explored for use in energy storage devices[98], sensors[59] and other components[63].

Conclusions and outlook

The existence of a recently developed, powerful set of capabilities in NM materials and assembly, taken together with multiple important and uniquely addressable application areas, provides excellent motivation for expanded activities in this rapidly emerging field. The possible topics for basic study are many, and include investigations of physical, chemical and transport properties at interfaces between heterogeneous, printed stacks of NMs; phenomena in the limit of ultrathin geometries where quantum confinement, interface depletion effects and molecular modification can be important; modified phonon and thermal characteristics for controlled heat flow in structured NMs; and strain engineering for spatially modulated bandgap properties.

For work in engineering, the most promising areas are in systems with operational features that cannot be achieved using established approaches. The overall device integration, as currently practiced, involves release of NMs from a source substrate, followed by assembly and final interconnection. This sequence is much different from the prevailing trend in conventional electronics, where individual devices, produced at the highest levels of interconnection possible on a semiconductor wafer, are diced and assembled as a terminal packaging step. The engineering challenges and balance of costs associated with the NM approach are important topics of research and development in manufacturing. An optimized process might incorporate a blend of strategies whereby, for example, some significant level of integration is accomplished on the NMs before their release and assembly, depending on the details of the application.

Techniques for synthesizing NMs are central to all future activities. New ideas are needed to expand the range of inorganic NM materials beyond those that can be achieved by known exfoliation, etching, epitaxial and bonding methods. As for other classes of nanomaterials, morphological and chemical properties of the surfaces of NMs are paramount. In some cases, existing technologies for surface passivation can be adapted to create multilayer NM structures, such as SiO_2/Si/SiO_2, that embed critical interfaces and isolate them from the environment. In others, these surfaces can be exposed and appropriately functionalized for applications in sensors. Progress on these and related topics will facilitate applications in fields inclusive of but wider ranging than electronics and optoelectronics, such as nanoelectromechanical devices, photonic/plasmonic structures, thermal and/or mechanical energy-harvesting elements, micro/nanoscale pressure sensors, micro/nanofluidic devices, molecular sensors, sieves, scaffolds for cell culture and others. Synthesis of functionally useful organic NMs is a persistent and notable challenge in chemistry, but one that now seems possible to address by interfacial assembly and crosslinking on monocrystalline substrates. For all classes of materials, understanding the physics of transport in shaped, chemically functionalized and/or strain-engineered NMs may lead to additional properties that lie beyond those that can be achieved otherwise.

Application opportunities seem to be particularly promising in bio-integrated systems, where many NM materials and structures might be combined in packages that establish and actively maintain intimate, dynamic interfaces with the body. In such cases, organic and inorganic NMs could function together, with the former at the bio-interface for sensing, exchanging materials and establishing bio-compatibility, and the latter separately located for the purposes of actuating, processing and transmitting data and providing power. The ability to engineer 'soft', elastic responses and 3D, curvilinear configurations in NMs with optimized nanoarchitectures on 'tissue-like' substrates will be essential to satisfying dimensional and mechanical requirements set by biological constraints. Understanding the nanomechanics of these hard–soft hybrid-material constructs, where the elastic moduli can differ by a factor of one million or more, will be necessary to allow precise physical matching to tissues. Recent advances, for example, demonstrate the ability to form NM electronics with the properties of the epidermis[99]. An ultimate goal might be systems based on man-made NMs that provide seamless, integrated functions in living systems, potentially rivalling those of naturally occurring NMs in biology. The interesting fundamental science, the diverse possibilities for creative engineering and the strong potential for broadly influential outcomes make this field of NM research a fertile one for future investigation.

1. Steigerwald, M. L. & Brus, L. E. Semiconductor crystallites — a class of large molecules. *Acc. Chem. Res.* **23,** 183–188 (1990).
2. Hebard, A. F. Buckminsterfullerene. *Annu. Rev. Mater. Sci.* **23,** 159–191 (1993).
3. Lu, W. & Lieber, C. M. Nanoelectronics from the bottom up. *Nature Mater.* **6,** 841–850 (2007).
4. Novoselov, K. S. Two-dimensional atomic crystals. *Proc. Natl Acad. Sci. USA* **102,** 10451–10453 (2005).
5. Osada, M. & Sasaki, T. Exfoliated oxide nanosheets: new solution to nanoelectronics. *J. Mater. Chem.* **19,** 2503–2511 (2009).
6. Ma, R. & Sasaki, T. Nanosheets of oxides and hydroxides: ultimate 2D charge-bearing functional crystallites. *Adv. Mater.* **22,** 5082–5104 (2010).
7. Hirsch, A. The era of carbon allotropes. *Nature Mater.* **9,** 868–871 (2010).
8. Diederich, F. & Kivala, M. All-carbon scaffolds by rational design. *Adv. Mater.* **22,** 803–812 (2010).
9. Sakamoto, J., van Heijst, J., Lukin, O. & Schlüter, A. D. Two-dimensional polymers: just a dream of synthetic chemists? *Angew. Chem. Int. Ed.* **48,** 1030–1069 (2009).
10. Kim, S. *et al.* Microstructured elastomeric surfaces with reversible adhesion and examples of their use in deterministic assembly by transfer printing. *Proc. Natl Acad. Sci. USA* **107,** 17095–17100 (2010).
11. Meitl, M. A. *et al.* Transfer printing by kinetic control of adhesion to an elastomeric stamp. *Nature Mater.* **5,** 33–38 (2005).
Report on deterministic assembly of micro/nanoscale objects with elastomeric stamps.
12. Lee, K. J. *et al.* Large-area, selective transfer of microstructured silicon: a printing-based approach to high-performance thin-film transistors supported on flexible substrates. *Adv. Mater.* **17,** 2332–2336 (2005).
13. Cavallo, F. & Lagally, M. G. Semiconductors turn soft: inorganic nanomembranes. *Soft Matter* **6,** 439–455 (2010).

14. Huang, M. *et al.* Nanomechanical architecture of strained bilayer thin films: from design principles to experimental fabrication. *Adv. Mater.* **17,** 2860–2864 (2005).
15. Li, X. L. Strain induced semiconductor nanotubes: from formation process to device applications. *J. Phys. D Appl. Phys.* **41,** 193001 (2008).
16. Schmidt, O. G. & Eberl, K. Thin solid films roll up into nanotubes. *Nature* **410,** 168–168 (2001).
Report on rolled-up tubes from initially flat NMs.
17. Ko, H. C. *et al.* Curvilinear electronics formed using silicon membrane circuits and elastomeric transfer elements. *Small* **5,** 2703–2709 (2009).
18. Sun, L. *et al.* 12-GHz thin-film transistors on transferrable silicon nanomembranes for high-performance flexible electronics. *Small* **6,** 2553–2557 (2010).
19. Ahn, J.-H. *et al.* Heterogeneous three-dimensional electronics by use of printed semiconductor nanomaterials. *Science* **314,** 1754–1757 (2006).
20. Yuan, H.-C. *et al.* Flexible photodetectors on plastic substrates by use of printing transferred single-crystal germanium membranes. *Appl. Phys. Lett.* **94,** 013102 (2009).
21. Viventi, J. *et al.* A conformal, bio-interfaced class of silicon electronics for mapping cardiac electrophysiology. *Sci. Transl. Med.* **2,** 24ra22 (2010).
Report on flexible NM electronics for mapping cardiac electrophysiology.
22. Symon, K. R. *Mechanics* 3rd edn (Addison-Wesley, 1971).
23. Kiefer, A. M. *et al.* Si/Ge junctions formed by nanomembrane bonding. *ACS Nano* **5,** 1179–1189 (2011).
24. Chen, F. *et al.* Quantum confinement, surface roughness, and the conduction band structure of ultrathin silicon membranes. *ACS Nano* **4,** 2466–2474 (2010).
25. Zhang, P. *et al.* Electronic transport in nanometre-scale silicon-on-insulator membranes. *Nature* **439,** 703–706 (2006).
Report on the influence of surfaces in controlling conduction in NMs.
26. Yu, J.-K., Mitrovic, S., Tham, D., Varghese, J. & Heath, J. R. Reduction of thermal conductivity in phononic nanomesh structures. *Nature Nanotechnol.* **5,** 718–721 (2010).
27. Tang, J. *et al.* Holey silicon as an efficient thermoelectric material. *Nano Lett.* **10,** 4279–4283 (2010).
28. Fujita, M., Takahashi, S., Tanaka, Y., Asano, T. & Noda, S. Simultaneous inhibition and redistribution of spontaneous light emission in photonic crystals. *Science* **308,** 1296–1298 (2005).
29. Siriani, D. F. *et al.* Mode control in photonic crystal vertical-cavity surface-emitting lasers and coherent arrays. *IEEE J. Sel. Top. Quantum Electron.* **15,** 909–917 (2009).
30. Coleman, J. N. *et al.* Two-dimensional nanosheets produced by liquid exfoliation of layered materials. *Science* **331,** 568–571 (2011).
31. Radisavljevic, B., Radenovic, A., Brivio, J., Giacometti, V. & Kis, A. Single-layer MoS_2 transistors. *Nature Nanotechnol.* **6,** 147–150 (2011).
32. Davis, G. D., Viljoen, P. E. & Lagally, M. G. Determination of shallow core level spectra in selected compound semiconductors. *J. Electron Spectrosc.* **20,** 305–318 (1980).
33. Baca, A. J. *et al.* Printable single-crystal silicon micro/nanoscale ribbons, platelets and bars generated from bulk wafers. *Adv. Funct. Mater.* **17,** 3051–3062 (2007).
34. Mack, S., Meitl, M. A., Baca, A. J., Zhu, Z. T. & Rogers, J. A. Mechanically flexible thin-film transistors that use ultrathin ribbons of silicon derived from bulk wafers. *Appl. Phys. Lett.* **88,** 213101 (2006).
35. Ko, H. C., Baca, A. J. & Rogers, J. A. Bulk quantities of single-crystal silicon micro-/nanoribbons generated from bulk wafers. *Nano Lett.* **6,** 2318–2324 (2006).
36. Yoon, J. *et al.* GaAs photovoltaics and optoelectronics using releasable multilayer epitaxial assemblies. *Nature* **465,** 329–333 (2010).
37. Yablonovitch, E., Gmitter, T., Harbison, J. P. & Bhat, R. Extreme selectivity in the lift-off of epitaxial GaAs films. *Appl. Phys. Lett.* **51,** 2222–2224 (1987).
38. Konagai, M., Sugimoto, M. & Takahashi, K. High efficiency GaAs thin film solar cells by peeled film technology. *J. Cryst. Growth* **45,** 277–280 (1978).
39. Stern, F. & Woodall, J. M. Photon recycling in semiconductor lasers. *J. Appl. Phys.* **45,** 3904–3906 (1974).
40. Park, S. I. *et al.* Printed assemblies of inorganic light-emitting diodes for deformable and semitransparent displays. *Science* **325,** 977–981 (2009).
41. Sapienza, L. *et al.* Cavity quantum electrodynamics with Anderson-localized modes. *Science* **327,** 1352–1355 (2010).
42. Matthews, J. W. & Blakeslee, A. E. Defects in epitaxial multilayers: I. Misfit dislocations. *J. Cryst. Growth* **27,** 118–125 (1974).
43. Menard, E., Lee, K. J., Khang, D. Y., Nuzzo, R. G. & Rogers, J. A. A printable form of silicon for high performance thin film transistors on plastic substrates. *Appl. Phys. Lett.* **84,** 5398–5400 (2004).
44. Huang, M., Cavallo, F., Liu, F. & Lagally, M. G. Nanomechanical architecture of semiconductor nanomembranes. *Nanoscale* **3,** 96–120 (2011).
45. Rogers, J. A., Someya, T. & Huang, Y. G. Materials and mechanics for stretchable electronics. *Science* **327,** 1603–1607 (2010).
Review of stretchable and curvilinear electronics based on shape-engineered NMs and other materials.
46. Moutanabbir, O. & Gösele, U. Heterogeneous integration of compound semiconductors. *Annu. Rev. Mater. Res.* **40,** 469–500 (2010).
47. Zhang, Y. *et al.* The fabrication of large-area, free-standing GaN by a novel nanoetching process. *Nanotechnology* **22,** 045603 (2011).
48. Kando, H. *et al.* in *Microwave Conf. Proc. (APMC), 2010 Asia-Pacific* 920–923 (IEEE, 2010).
49. Liu, Z., Wu, J., Duan, W., Lagally, M. & Liu, F. Electronic phase diagram of single-element silicon ''strain'' superlattices. *Phys. Rev. Lett.* **105,** 016802 (2010).
50. Euaruksakul, C. *et al.* Influence of strain on the conduction band structure of strained silicon nanomembranes. *Phys. Rev. Lett.* **101,** 147403 (2008).
51. Scott, S. A. & Lagally, M. G. Elastically strain-sharing nanomembranes: flexible and transferable strained silicon and silicon–germanium alloys. *J. Phys. D.* **40,** R75–R92 (2007).
52. Roberts, M. M. *et al.* Elastically relaxed free-standing strained-silicon nanomembranes. *Nature Mater.* **5,** 388–393 (2006).
Report on strain engineering in NMs, to achieve unique electronic properties.
53. Yuan, H.-C., Ma, Z., Roberts, M. M., Savage, D. E. & Lagally, M. G. High-speed strained-single-crystal-silicon thin-film transistors on flexible polymers. *J. Appl. Phys.* **100,** 013708 (2006).
54. Huang, M. *et al.* Mechano-electronic superlattices in silicon nanoribbons. *ACS Nano* **3,** 721–727 (2009).
55. Paskiewicz, D. M., Tanto, B., Savage, D. E. & Lagally, M. G. Defect-free single-crystal SiGe: a new material from nanomembrane strain engineering. *ACS Nano* **5,** 5814–5822 (2011).
56. Paskiewicz, D. M., Scott, S. A., Savage, D. E., Celler, G. K. & Lagally, M. G. Symmetry in strain engineering of nanomembranes: making new strained materials. *ACS Nano* **5,** 5532–5542 (2011).
57. Sanchez-Perez, J. R. *et al.* Direct-bandgap light-emitting germanium in tensilely strained nanomembranes. *Proc. Natl Acad. Sci. USA* (submitted).
58. Huang, G. S., Mei, Y. F., Thurmer, D. J., Coric, E. & Schmidt, O. G. Rolled-up transparent microtubes as two-dimensionally confined culture scaffolds of individual yeast cells. *Lab Chip* **9,** 263–268 (2009).
59. Bernardi, A. *et al.* On-chip Si/SiO_x microtube refractometer. *Appl. Phys. Lett.* **93,** 094106 (2008).
60. Kim, D.-H. *et al.* Stretchable and foldable silicon integrated circuits. *Science* **320,** 507–511 (2008).
61. Kim, D. H., Xiao, J. L., Song, J. Z., Huang, Y. G. & Rogers, J. A. Stretchable, curvilinear electronics based on inorganic materials. *Adv. Mater.* **22,** 2108–2124 (2010).
62. Timoshenko, S. Analysis of bi-metal thermostats. *J. Opt. Soc. Am.* **11,** 233–255 (1925).
63. Chun, I. S., Bassett, K., Challa, A. & Li, X. Tuning the photoluminescence characteristics with curvature for rolled-up GaAs quantum well microtubes. *Appl. Phys. Lett.* **96,** 251106 (2010).
64. Prinz, V. & Golod, S. Elastic silicon-film-based nanoshells: formation, properties, and applications. *J. Appl. Mech. Tech. Phys.* **47,** 867–878 (2006).
65. Geim, A. K. & Novoselov, K. S. The rise of graphene. *Nature Mater.* **6,** 183–191 (2007).
66. Tahara, K., Yoshimura, T., Sonoda, M., Tobe, Y. & Williams, R. V. Theoretical studies on graphyne substructures: geometry, aromaticity, and electronic properties of the multiply fused dehydrobenzo[12]annulenes. *J. Org. Chem.* **72,** 1437–1442 (2007).
67. Haley, M. M. Synthesis and properties of annulenic subunits of graphyne and graphdiyne nanoarchitectures. *Pure Appl. Chem.* **80,** 519–532 (2008).
68. Long, M., Tang, L., Wang, D., Li, Y. & Shuai, Z. Electronic structure and carrier mobility in graphdiyne sheet and nanoribbons: theoretical predictions. *ACS Nano* **5,** 2593–2600 (2011).
69. Diederich, F. Carbon scaffolding: building acetylenic all-carbon and carbon-rich compounds. *Nature* **369,** 199–207 (1994).
70. Schultz, M. J. *et al.* Synthesis of linked carbon monolayers: films, balloons, tubes, and pleated sheets. *Proc. Natl Acad. Sci. USA* **105,** 7353–7358 (2008).
71. Zheng, Z. *et al.* Janus nanomembranes: a generic platform for chemistry in two dimensions. *Angew. Chem. Int. Ed.* **49,** 8493–8497 (2010).
72. Geyer, W. *et al.* Electron-induced crosslinking of aromatic self-assembled monolayers: negative resists for nanolithography. *Appl. Phys. Lett.* **75,** 2401–2403 (1999).
73. Turchanin, A. *et al.* One nanometer thin carbon nanosheets with tunable conductivity and stiffness. *Adv. Mater.* **21,** 1233–1237 (2009).
74. Cai, J. M. *et al.* Atomically precise bottom-up fabrication of graphene nanoribbons. *Nature* **466,** 470–473 (2010).
Report on substrate-templated synthetic routes to graphene-like nanoribbons and NMs.
75. Zwaneveld, N. A. A. *et al.* Organized formation of 2D extended covalent organic frameworks at surfaces. *J. Am. Chem. Soc.* **130,** 6678–6679 (2008).
76. Colson, J. W. *et al.* Oriented 2D covalent organic framework thin films on single-layer graphene. *Science* **332,** 228–231 (2011).
77. Stankovich, S. *et al.* Synthesis of graphene-based nanosheets via chemical reduction of exfoliated graphite oxide. *Carbon* **45,** 1558–1565 (2007).
78. Hernandez, Y. *et al.* High-yield production of graphene by liquid-phase exfoliation of graphite. *Nature Nanotechnol.* **3,** 563–568 (2008).
79. Wu, J., Pisula, W. & Müllen, K. Graphenes as potential material for electronics. *Chem. Rev.* **107,** 718–747 (2007).
80. Dikin, D. A. *et al.* Preparation and characterization of graphene oxide paper. *Nature* **448,** 457–460 (2007).
81. Xu, Y., Bai, H., Lu, G., Li, C. & Shi, G. Flexible graphene films via the filtration of water-soluble noncovalent functionalized graphene sheets. *J. Am. Chem. Soc.* **130,** 5856–5857 (2008).
82. Green, A. A. & Hersam, M. C. Solution phase production of graphene with controlled thickness via density differentiation. *Nano Lett.* **9,** 4031–4036 (2009).
83. Sasaki, D. Y., Carpick, R. W. & Burns, A. R. High molecular orientation in mono- and trilayer polydiacetylene films imaged by atomic force microscopy. *J. Colloid Interf. Sci.* **229,** 490–496 (2000).
84. Whang, D., Jin, S., Wu, Y. & Lieber, C. M. Large-scale hierarchical organization of nanowire arrays for integrated nanosystems. *Nano Lett.* **3,** 1255–1259 (2003).
85. Knuesel, R. J. & Jacobs, H. O. Self-assembly of microscopic chiplets at a liquid-liquid-solid interface forming a flexible segmented monocrystalline solar cell. *Proc. Natl Acad. Sci. USA* **107,** 993–998 (2010).
86. Menard, E., Nuzzo, R. G. & Rogers, J. A. Bendable single crystal silicon thin film transistors formed by printing on plastic substrates. *Appl. Phys. Lett.* **86,** 093507 (2005).

87. Bae, S. *et al.* Roll-to-roll production of 30-inch graphene films for transparent electrodes. *Nature Nanotechnol.* **5,** 574–578 (2010).
88. Scott, S. A., Paskiewicz, D. M., Savage, D. E. & Lagally, M. G. Silicon nanomembranes incorporating mixed crystal orientations. *ECS Trans.* **16,** 215–218 (2008).
89. Unarunotai, S. *et al.* Layer-by-layer transfer of multiple, large area sheets of graphene grown in multilayer stacks on a single SiC wafer. *ACS Nano* **4,** 5591–5598 (2010).
90. Unarunotai, S. *et al.* Transfer of graphene layers grown on SiC wafers to other substrates and their integration into field effect transistors. *Appl. Phys. Lett.* **95,** 202101 (2009).
91. Ko, H. C. *et al.* A hemispherical electronic eye camera based on compressible silicon optoelectronics. *Nature* **454,** 748–753 (2008).
92. Yuan, H.-C., Celler, G. K. & Ma, Z. 7.8-GHz flexible thin-film transistors on a low-temperature plastic substrate. *J. Appl. Phys.* **102,** 034501 (2007).
93. Kim, R.-H. *et al.* Waterproof AlInGaP optoelectronics on stretchable substrates with applications in biomedicine and robotics. *Nature Mater.* **9,** 929–937 (2010).
94. Lee, K. J. *et al.* Bendable GaN high electron mobility transistors on plastic substrates. *J. Appl. Phys.* **100,** 124507 (2006).
95. Yuan, H.-C., Qin, G., Celler, G. K. & Ma, Z. Bendable high-frequency microwave switches formed with single-crystal silicon nanomembranes on plastic substrates. *Appl. Phys. Lett.* **95,** 043109 (2009).
96. Ko, H. *et al.* Ultrathin compound semiconductor on insulator layers for high-performance nanoscale transistors. *Nature* **468,** 286–289 (2010).
Report on transistors using NMs of InAs printed onto silicon substrates.
97. Li, F. & Mi, Z. T. Optically pumped rolled-up InGaAs/GaAs quantum dot microtube lasers. *Opt. Express* **17,** 19933–19939 (2009).
98. Ji, H.-X. *et al.* Self-wound composite nanomembranes as electrode materials for lithium ion batteries. *Adv. Mater.* **22,** 4591–4595 (2010).
99. Kim, D. H. *et al.* Epidermal electronics. *Science* **333,** 838 (2011).
Report on NM electronics with mechanical properties matched to the epidermis, for skin-mounted devices.

Acknowledgements We thank F. Du, A.-P. Le and S. Jo for assistance. The preparation of this manuscript was supported by a National Security Science and Engineering Faculty Fellowship and by AFOSR through a Multidisciplinary University Research Initiative grant (FA9550-08-1-0337). Work described in this Review that was performed by the authors was supported by the US DOE (DE-FG02-03ER46028, DE-FG02-07ER46471, DE-FG36-08GO18021 and DE-FG02-07ER46453), the US NSF/MRSEC programme (DMR-0520527), the US AFOSR (FA9550-08-1-0337) and the US NSF (DMI-0328162).

Author Contributions J.A.R. led the preparation of the manuscript, wrote the sections 'Single- and multilayer assembly', 'Applications in electronics and optoelectronics' and 'Conclusions and outlook', and assembled the figures. M.G.L. and J.A.R. wrote the section 'Inorganic nanomembranes'. R.G.N. and J.A.R. wrote the section 'Organic nanomembranes'. All three authors contributed to the introduction and to editorial modifications of the overall text.

Author Information Reprints and permissions information is available at www.nature.com/reprints. The authors declare no competing financial interests. Readers are welcome to comment on the online version of this article at www.nature.com/nature. Correspondence should be addressed to J.A.R. (jrogers@illinois.edu).